



HAL
open science

Testing the Boolean hypothesis in the non-convex case when a bounded grain can be assumed

Joël Chadoeuf, Jean-Noël Bacro, Gael Thébaud, Gérard Labonne

► **To cite this version:**

Joël Chadoeuf, Jean-Noël Bacro, Gael Thébaud, Gérard Labonne. Testing the Boolean hypothesis in the non-convex case when a bounded grain can be assumed. *Environmetrics*, 2008, 19 (2), pp.123-136. 10.1002/env.860 . hal-02659993

HAL Id: hal-02659993

<https://hal.inrae.fr/hal-02659993v1>

Submitted on 30 May 2020

HAL is a multi-disciplinary open access archive for the deposit and dissemination of scientific research documents, whether they are published or not. The documents may come from teaching and research institutions in France or abroad, or from public or private research centers.

L'archive ouverte pluridisciplinaire **HAL**, est destinée au dépôt et à la diffusion de documents scientifiques de niveau recherche, publiés ou non, émanant des établissements d'enseignement et de recherche français ou étrangers, des laboratoires publics ou privés.

Postprint

Version définitive du manuscrit publié dans / Final version of the manuscript
published in : Environmetrics, 2008, vol.19, no.2, 123-136

Testing the boolean hypothesis in the non convex case when a bounded grain can be assumed

Chadoëuf*J, Bacro[†] JN, Thébaud[‡] G & Labonne[‡] G.

short title : testing the boolean hypothesis in the non convex case.

*INRA Biométrie, Site Agroparc, 84914 Avignon Cedex 9, FRANCE
email : *joel@avignon.inra.fr*
tel : 04-32-72-21-76
fax : 04-32-72-21-82

[†] I3M, UMR CNRS 5149, Université Montpellier II,
Place E. Bataillon, 34095 Montpellier Cedex 5, FRANCE

[‡] UMR BGPI, TA 41/K, 34398 Montpellier Cedex 5, FRANCE

Postprint

Version définitive du manuscrit publié dans / Final version of the manuscript
published in : Environmetrics, 2008, vol.19, no.2, 123-136

summary: Spatial independence of objects is a strong hypothesis when using Boolean models. Methods to test it have then been developed, but only when the objects are convex. We propose here to replace this assumption by a bound assumption of the objects which can be more easily assumed when modeling spatial patterns in ecology and agricultural science. A test is then proposed, based on the length of the voids of the intersection between transect lines and a dilation of the original process related to the bound value. Its application is shown to several examples, together with its extension to an epidemiological case on orchards, where this problem comes from.

key-words: area, boolean model, spatial pattern

introduction

Boolean models are used in spatial statistics to model the spatial repartition of objects. They assume that these objects, generally called grains, are independently located and have independent shapes. The boolean model is then obtained as the union of all these objects. Boolean models are used in very different fields as for example in ecology where they can be used to describe the spatial repartition of plants when these plants cannot be assumed punctual (Diggle 1981), or in soil science when modeling the soil surface roughness (Bertuzzi et al 1995, Kamphorst et al 2005), this surface being considered as the union of independent 3D shapes, the easiest one being the half-sphere.

A less classical case can be encountered in spatial epidemiology when looking at diseases transmitted by insects on regularly planted plots. For exemple, European stone fruit yellows (ESFY) is a disease affecting apricot orchards, where it is transmitted by an insect species (*Cacopsylla pruni*) that spends only a short part of its life cycle in the orchards and lives mostly on pine trees several kilometers away (Thébaud 2005). Phytoplasmas can be transmitted only after spending several weeks inside their insect vector; in the case of ESFY, the healthy insects landing onto an infectious tree can acquire the phytoplasma but they do not spend enough time in the apricot orchards to become infectious before disappearing (Thébaud 2005). Therefore, only the insects that are already infectious when they arrive into the orchard from distant pine trees are responsible for contaminating the apricot trees. Moreover suppose that, once this large flight from pine trees to the orchards is done, the insects perform only a few flights at short distance (to the nearest trees or the next ones), unless they are disturbed in which case they will perform very large ones. Assuming independence of insects, i.e. that they arrive independently to each other and independently to trees already carrying ESFY, the pattern of ESFY trees can be considered as the sampling of a boolean process. In this boolean process each object is formed by the union of the surfaces formed by meshes centered on the successive insect positions on the crown, supposed to cover all the orchard area. For young trees whose crowns do not connect, the same applies if one can assume that the arrival point process is Poisson on the area formed by the union of the tree crowns.

In all these cases, independence hypothesis is a crucial assumption as it influences all statistical properties of the model. Testing it is then a preliminary step before going to spatial modeling when only global statistical

Postprint

Version définitive du manuscrit publié dans / Final version of the manuscript
published in : Environmetrics, 2008, vol.19, no.2, 123-136

properties are of interest, or an important step for itself in cases like plant epidemiology as it can give some insight into insect behavior, which is difficult to observe directly.

Such a test has been developed by Laslett (Laslett *et al.* 1985, Cressie 1991, Molchanov 1997). It is based on the analysis of the spatial pattern of observed extrema. It remains thus very general, the only needed assumption being that of convexity. On the other side, this assumption is seldom met in agricultural science and ecology where convexity assumption can be more easily replaced by other assumptions as for example boundedness of the grain, on the basis of biological knowledge. In the ESFY example given above, a grain is the union of plants contaminated by one insect and will not generally be convex. Field observations on insect behavior can lead to a maximum number of short distance flights and a maximum distance of flight, and the bound will be given by the product of the two parameters. In ecology, boolean models can be used to describe the spatial repartition of plants whose crown can be observed. The underlying assumption is then that seedlings are independently spread and grow independently, a bush being an isolated plant or the union of several plants with connected crowns. In general, the crown of one plant is not convex, except for some species with very regular growth.

As mentioned by Molchanov (1997), testing the boolean hypothesis without any assumption on the grain is impossible, and we propose here to replace the convexity assumption by a boundedness condition. The principle of the test, presented in section one, is first to dilate the process in one dimension, then to sample transect lines parallel to that direction and compare the length distribution of voids with the expected distribution of voids under the assumption of total randomness conditional on the number of segments and the total void length. In section two we show how the test works on three simulated examples, where the typical point process is successively a Poisson point process, a Strauss process and an aggregated point process. In section three we apply the test on two examples, one from soil surfaces description, the second from ecology and interested in box (*Buxus sempervirens*) bushes distribution. In section four, we show how the test can be adapted to the example of ESFY epidemics, and how finiteness of the orchards can be dealt with. Limits of the method will be discussed in a last section.

1 The boolean model in \mathbf{R}^2

1.1 The boolean model

Definition of the boolean model can be found in (Cressie 1991, Hall 1988, Molchanov 1997, Stoyan 1995) together with an extensive description of its properties. We just recall here its definition.

Let $X = (X_i)_{i \in \mathbf{N}}$, an homogeneous Poisson point process and $M = (M_i)_{i \in \mathbf{N}}$ a set of measurable independent random sets. For b a bounded set, let $S_b = S \oplus b$ denote the dilation of S by b . The boolean model $B = (X, M)$ is defined as $B = \bigcup_i X_i \oplus M_i$. In the following, we assume that the grains are bounded, that is, there exists $0 < r < \infty$ so that $M_i \in A(0, r)$, the disk of center O and radius r .

Note that the dilation of B , $B_b = B \oplus b = \bigcup_i X_i \oplus (M_i \oplus b)$, is also a boolean process. Therefore, if B is a boolean process with bounded grain, the process obtained by dilating each grain by a disk of radius r (resp. by an oriented segment of length r) is a boolean process. In the first case, the intersection of any dilated grain by a given line D is a segment. In the second case, the intersection of any dilated grain by a given line D parallel to the dilating segment is also a segment.

1.2 the intersection of a boolean model by a straight line

If D is a given straight line, the intersection $B \cap D$ of the boolean process B by D is a boolean process. This can be easily understood in the case of bounded grains: grains $X_i \oplus M_i$ intersecting D have their typical point X_i in a cylinder C of width $2r$ and axe parallel to D . $B \cap D$ is then equal to $\bigcup P(X_i) \oplus M_i \cap D$ where P is the orthogonal projection of C onto D . Therefore, the intersection by a line D of the dilation of the bounded boolean process by a segment of length r parallel to D is a boolean process of segments. If D_i is a series of parallel lines separated by more than r , the boolean processes B_i defined as the intersections with the lines D_i of the dilation of B by the segment of length r parallel to D_0 are independent.

If B_0 is a boolean segment process on the lines, let us denote V_i the void segments, that is the segments not intercepting B_0 . The length l_i of the void

segments are independent and exponentially distributed. So, the length distribution of the n segments V_i , knowing that $\sum_{i=1}^n l_i = L$, is the distribution of segments obtained by throwing $n - 1$ points uniformly independently on a segment of length L .

1.3 The proposed test

Let $B \cap W$ be the observation of the boolean process B through a rectangular sampling window $W = [0, a] \times [0, b]$. Suppose that the grains of the boolean process are bounded by a positive bound r .

We propose in a first step to dilate the observed process by the segment $[0, r]$ parallel to one of the sides of W , say the first one, then restrict the observation of the dilated process to the window $W_r = [r, a] \times [0, b]$ so as to avoid border effect.

In a second step, we consider a series of N parallel transects D_i , parallel to the first side of W , and separated by r . The K intersections $D_i \cap B_r \cap W_r$ are then K independent realizations of a boolean segment process on the line observed through a segment of length $a - r$.

In a third step, we consider the lengths $l_{i,j}$ $j \leq J_i$ of the J_i void segments of $D_i \cap B_r \cap W_r$ which do not intercept the border of W_r .

Under the boolean assumption, the distribution of the $(l_{i,j})$ lengths knowing the total length of J_i uncensored void segments per transect $L_i = \sum_{j=1}^{J_i} l_{i,j} > 0$ is the distribution of length of the consecutive segments obtained by throwing $J_i - 1$ points randomly uniformly on the segments L_i .

The statistics that we propose to use is then the length distribution of void segments $g(x, (l_{i,j})) = \frac{1}{\sum_{i=1}^N J_i} \sum_{i=1}^N \sum_{j=1}^{J_i} \mathbf{1}_{\{l_{i,j} \leq x\}}$

The test can be performed by either:

- comparing the observed statistics to its individual confidence band, obtained by simulation,
- computing the p-value of the observed segment length variance.

A detailed description of such type of procedure can be found for example in Diggle (1981) in the case of mapped point pattern exploration.

1.4 Grid approximation

In practice, one very often does not observe the area process in W , but observe its realization on a regular grid, the realization at the center of each cell being 1 or 0 whether the cell intersects the boolean process or not. Let $S \subset \mathbb{Z}^2$ a set of indices describing the node number. Let $U = (u_s)_{s \in S}$ be the intersection of the grid with W , $v_s = \{x \in W; \|x - u_s\| = \min_{s'}(\|x - u_{s'}\|)\}$ the neighbourhood of node u_s .

Consider for example the case of bush coverage mapping by using aerial photography, as presented in the next section. The observed process is then $X = (x_s)_{s \in S}$, where $x_s = \mathbf{1}_{\{v_s \cap B \neq \emptyset\}}$ that is the value of the pixel is 1 as soon as the neighbourhood v_s of the node u_s intercepts the bush pattern.

This can be also the case when looking at a plant disease transmitted by insects in orchards. Suppose that the trees are old enough so that their crowns form a continuous surface. Trees being of the same age, species and cultivar, the crowns of all trees are more or less similar, and equal to v_0 , the area of the cell centered at 0, as soon as they do not overlap. If insects arrive and move independently in the crown, let us denote Y_i the position of insect i at its arrival in the orchard, $Z_i = \cup_{j \in J_i} u_{ij}$ the set of its successive relative positions from Y_i . The sets $Y_i \oplus Z_i$ are independent from each other. If insects arrive in independent identically distributed small groups, let Y_i be the center of a group, Z_i the relative positions of insects of group i around Y_i . Then, one gets also that the sets $Y_i \oplus Z_i$ are independent from each other. Let us attach v_0 , the surface of the pixel of the orchard grid, at all insect landings. The corresponding area process $B = \cup_i (Y_i \oplus Z_i \oplus v_0)$ is a boolean process. Suppose that while feeding on trees these insects transmit a disease observed at the tree level. The observed process of diseased tree X is then the intersection of U with the boolean process B .

In all these cases, if the value of X_{s_1}, \dots, X_{s_n} on n consecutive points of the grid is null, then the intersection of the original boolean process with the segment $[X_{s_1}, X_{s_n}]$ is empty, and two consecutive empty segments on the grid are of independent length. The same tests as above can be applied by replacing randomness of segment limits on $[0, L_i]$ by randomness of segment limits on $[0, L_i] \cap \mathbb{N}$ and conditioning on the number of segments.

2 Simulation examples

Two simulated examples were performed in order to check the procedure. In the first one, we used a boolean model with non-convex grains to see if the boolean hypothesis was not rejected when taking into account the non-convexity as proposed above, and rejected if not taken into account. In the second one, we considered a Strauss point process, on which we attached the same non-convex grains, in order to test if the boolean hypothesis was rejected when taking into account the non-convexity.

2.1 Boolean model

Figure 1(a) presents a realization of the boolean model . The Poisson process intensity is $\lambda = 24.3$, each grain is formed of 3 discs of radius $r = 0.044$ disposed on an horizontal line and separated by a distance $d = 0.066$. The process is observed on a 5×5 window.

Bound was chosen equal to $b = 0.244$, distance between consecutive horizontal transects was equal to b . Figure 1(b) illustrates the result of the dilation on the original process observed on the intersection with the transects and W_r .

Figure 1(c) presents the result of the test when no dilation of the original process is performed. The observed segment length distribution remains generally outside the individual confidence band, leading to a rejection of the boolean hypothesis. Similarly, the thick line representing the p-value $p(x)$ remains below 5%.

Figure 1(d) presents the result of the test after dilation. The observed segment length distribution is presented in thin plain line with its 95% individual confidence band in broken line. The observed curve lies inside its individual confidence band under the boolean hypothesis. The thick broken line presents the changes of the p-value $p(x)$. This last function is never below 0.42, corresponding to no rejection of the boolean hypothesis.

In this case, not taking into account the non-convexity may lead to falsely reject the boolean hypothesis.

2.2 Strauss model of typical points

The Strauss model used was defined with the following parameters. Point process intensity was $\lambda = 24.3$, inhibition parameter $c = 0.5$ and inhibition

distance $r = 0.44$. The grains attached to each point have same characteristics as above. Observation window was a 5×5 square. For testing, the bound was chosen equal to $b = 0.244$ and the distance between consecutive horizontal transects was equal to b .

Figure 2(a) presents a realization of the process, figure 2(b) the result of the dilation of this realization observed on the intersection with the transects.

Figure 2(c) presents the result of the test when no dilation is performed. The observed segment length distribution lies outside the individual confidence band build under H_0 , its p-value function being always near 0, so that the boolean hypothesis is rejected. However, rejection is not so much due to a lack of short length segments as expected from the Strauss process, but to an excess due to the grain non-convexity. Not taking into account the grain shape but just looking at such curves may then lead to misinterpretations, as for example concluding the typical point process is not Poisson but an aggregative process instead of a regular one.

Figure 2(d) presents the result of the test after dilation of the original process. The observed segment length lies outside the confidence band for short lengths, leading to rejection of the boolean hypothesis, but the curve lies near the limits of the confidence bound.

From the test procedure itself, in the case of a regular process, large void segments appear less often than expected under the boolean assumption. The same result should also be true for small segments but, because of the non-convexity, a grain could give several small void segments. In other words, ignorance of the non-convexity of the grain could then introduce a balancing of the small segments distribution and thus lead to a false conclusion regarding the underlying process. In such a case, taking into account the non-convexity of the grain is essential.

2.3 Test power

Two series of tests were conducted in order to look at changes in the power of the test. A first series was based on a Poisson distribution of typical points, a second one on a Strauss distribution. For each of them, point process characteristics were the same as above: $\lambda = 24.3$ in both cases and $c = 0.5$, $r = 0.44$ for the Strauss process.

We made vary i)the window area (5×5 , 10×10 , 15×15) in order to look at how the mixing property well applied to the tests results, and ii)the

distance between circles in order to look at the effect of the non-convexity of the grain ($d = k * 0.066$ with $k = 1 \dots 4$). The bound used in the test varied consequently. 100 simulations were performed in each case. The statistic used is the p-value of the segment length variance, which follows a uniform distribution under the boolean hypothesis.

Figure 3 presents the results in Q-Q plots. The curves corresponding to the boolean process are given in broken lines, those for the area process based on Strauss distribution in black lines. The thicker the line, the larger the distance between consecutive circles in one grain, the more the non convexity.

For a boolean model, Q-Q plot curves (in broken line) stay well around the diagonal curve. The larger the window, the closer the set of curves corresponding to a lower variability in the test. For a Strauss model, the larger the window, the better the test power for all distances d between consecutive circles. For the smaller window, the test is not powerful for the largest d ($d = 0.198$ and $d = 0.264$). In fact, for such d , the bound used becomes large and the coverage by the dilated grain is high, so that the number of segments at our disposal to perform the test drops.

3 Data set examples

3.1 Soil surface modeling

An experiment was conducted in INRA to study small scale roughness measurement techniques and modeling. Roughness is an important factor in soil surface as it greatly influences water storage and runoff. Several models have been proposed to model this roughness, among them boolean processes which offer the advantage of addressing explicitly the notion of clods, which are represented as union of grains.

In this case, soil clods were arranged on two areas, 1 square meter each, one in a seemingly random manner, the other one in rows of about 25 cm. Surface height was measured on a squared grid of 2mm lag by a automated laser device. Figures 4a and 4b present the area processes obtained by looking at part of the process above 10 cm height, after removal of the trend due to rows in the second case. Under boolean 3-D surface hypothesis, this area process is a boolean process.

The bound was taken as equal to 0.08 m. Figures 4a and 4b present the two process areas, Figures 5a and 5b the cumulative distribution function of

the segment length of the intersection of the dilated process by the horizontal transects. One may notice an excess of small segments with respect to the boolean hypothesis in the isotropic case, a lack of such segments in the anisotropic case. Interestingly, the test based on the variance of the segment length rejects boolean hypothesis in the anisotropic case ($p\text{-value}=0.018$), whereas it does not in the isotropic one ($p\text{-value}=0.16$), due to the distribution of large segments. From a modelling point of view, the isotropic surface can be modelled by a boolean process, whereas a boolean process cannot be used for anisotropic surfaces. In this last case, the undulations due to the ploughing lead to different radius clod distributions whether we look at them in the upper and lower parts of the undulation, or in between which presents smaller clods.

3.2 Spatial repartition of bushes

Box (*Buxus sempervirens*) bushes develop on former pasture areas unused for several years in regions like Causse Méjean in France, from where the picture presented in figure 4c is taken. *Buxus* is a slow growing plant which is invading these pastures since 50 years due to changes in agricultural practices. The invasion is caused by both bush expansion and seed spread (Rousset *et al* 2004).

In this picture, bushes more than 30 cm thick are shown and constitute the initial source of seeds on which dispersion models are applied. For a given box coverage, invasion speed will then depend on the spatial repartition of the seed sources. Mapping the bushes on large scales is not possible, and one has to rely on bush spatial repartition models, together with local measurements at several places to take into account possible large scale intensity variations. Knowing whether a boolean model is an acceptable model or whether a more specific one is necessary is a preliminary step to invasion prediction before deciding which kinds of measurements have to be done.

The observed pasture field (Figure 4c) is $130\text{m}\times 160\text{m}$. The bound was taken as equal to 9m, largely above the increase in thickness of *buxus* during 50 years (the estimated annual growth of box bushes in this region is 1cm/year in each direction). Such a large bound allowed for presence of some large bushes 50 years ago for agricultural practices as for example field delimitation or litter for sheep.

Figure 5b presents the segment length distribution curve. The curve lies inside the confidence band, near the upper limit. The test based on variance

of these lengths rejects the boolean hypothesis with a p-value of 0.001.

3.3 plant disease epidemiology

Figure 6a presents the health status of apricot trees in five young orchards, planted in 1999, where ESFY is present in southeastern France. The total number of trees is 5794 and the total number of diseased trees is 231. The distance between consecutive planting rows is 6 m and the distance between consecutive trees is 3 m. ESFY observation was made in 2004.

Figure 6b illustrates the inter-event distance computed on diseased trees, together with its confidence band at level 95% under independence hypothesis, conditional on the number of diseased trees in each orchard. Independence hypothesis is rejected in favour of an aggregative pattern of diseased trees. The vector of ESFY is a 2 mm long insect, *Cacopsylla pruni*, who transmits the disease during feeding. After a long flight it arrives in orchards at very low densities, but it tends to leave the orchard quite quickly as the apricot trees are not its preferred host plants for reproducing. From several field observations, for example during insect capture experiments, it was noted that these insects move mainly at short distance, or tend to go far away when disturbed. The hypothesis we want to test then is that insects do not interact. Under these assumptions the pattern of ESFY should be the result of the addition of individual independent patches, each patch corresponding to the successive tree infections by a given insect. To test it, we performed the proposed test, assuming that the diameter is less than 4 consecutive trees (12 m). The result of the test is shown in Figure 6c. The observed curve lies well inside the confidence band and the hypothesis is not rejected.

4 conclusion

Testing independence assumptions between objects needs various solutions depending on the properties of the observations. If each object can be completely observed and distinguished from the other ones, specific approaches to test independence assumptions can be applied, as for example that of Wiegand *et al.* 2006. When the result of the objects superposition only is observed, as this is generally the case with boolean models, such methods cannot be used. Other methods have then to be applied, as for example

the one we propose to test the boolean hypothesis in the case of non-convex grains.

Contrarily to the approach proposed by Molchanov(1997), we do not need an asymptotic approach but we have to rely on an boundedness assumption of the grain. It can be noted that the same assumption is necessary for its intensity estimation (Schmitt 1991).

The proposed method relies on filling in the empty spaces inside a grain along horizontal lines, so as to obtain a classical convex boolean model on the line. Molchanov's proposal, dilation of the boolean model, then applying Laslett transform and checking for Poisson hypothesis of the translated tangence points relies through the dilation on the same idea : completing the empty spaces inside the grain. However, the dilation being then done in all directions, the proportion of points covered by the dilated process is heavier, as one has to ensure that all the dilated grains are more or less convex. Moreover, even if a bound of the grain is known, no insurance is given how much the final grain is near convexity. Dilating a star with five long branches is a typical example in this case.

More and more data sets are acquired by automatic devices, where data are given as images. In such cases and for convex grains, it can be very difficult to locate a tangence point if the convexity radius is large. As a consequence, tangence point locations are often subject to errors. How these ones will affect the transformation is unknown but clearly errors add up. Applying Laslett transform on dilated images of the original process is then not so easy and needs to find an acceptable compromise between a large dilation, necessary to approach convexity, and a small dilation, to keep a convexity radius small enough with respect to the pixel size. The method we propose avoids the necessity of such a compromise, which is difficult to accept in practice.

References

- BERTUZZI P., GARCIA-SANCHEZ L., CHADGEUF J., GUERIF J., GOULARD M. & MONESTIEZ P. 1995. Modelling surface roughness by a boolean approach. *EJSS* 46, 215-220.
- CRESSIE N. 1991. *Statistics for Spatial Data*. Wiley, New-York.
- DIGGLE P. 1981. Binary mosaics and the spatial pattern of heather. *Bio-metrics*, 37, 531-539.

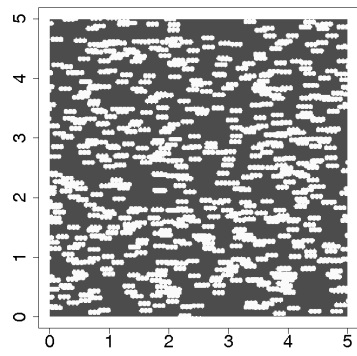
Postprint

Version définitive du manuscrit publié dans / Final version of the manuscript
published in : *Environmetrics*, 2008, vol.19, no.2, 123-136

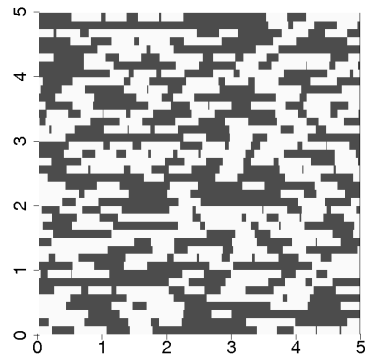
- HALL P. 1988. *Introduction to the theory of coverage processes*. Wiley, New-York.
- KAMPHORST E.C. , CHADŒUF J. , JETTEN V. & AND GUÉRIF J. 2005. Generating 3D soil surfaces from 2D height measurements to determine depression storage. *Catena* 62, 2-3, 189-205.
- LASLETT G.M., CRESSIE N. & LIOW S. 1985. Intensity estimation in a spatial model of overlapping particles. Unpublished manuscript, Division of Mathematics and Statistics, CSIRO, Melbourne.
- MOLCHANOV I. 1997. *Statistics of the Boolean Model for Practitioners and Mathematicians*. Wiley, New-York.
- ROUSSET O., CHADŒUF J., LEPART J. & MONESTIEZ P. 2004. Embroussaillement des parcours: processus biologiques de la régénération du buis et patrons locaux de répartition spatiale. *in Organisation spatiale des activités agricoles et processus environnementaux*, Monestiez Ed., Paris.
- SCHMITT M. 1991. Estimation of the density in a stationary Boolean model. *J. Appl. Proba.*, 28,, 702-708.
- STOYAN D., KENDALL W.S. & MECKE J. 1995. *Stochastic geometry and its applications* Wiley, New-York.
- THÉBAUD G. 2005. Etude du développement spatio-temporel d'une maladie transmise par vecteur en intégrant modélisation statistique et expérimentation : cas de l'ESFY (European stone fruit yellows). Thèse de l'Ecole Nationale Supérieure Agronomique de Montpellier.
- WIEGAND T., KISSLING W.D., CIPRIOTTI, P.A. & AGUIAR M.R. 2006. Extending point pattern analysis for objects of finite size and irregular shape. *J. of Ecology*, 94, 825-837.

List of Figures

- **Figure 1:** (a) realization of a boolean process with Poisson intensity 24.3, each grain being the union of three discs of radius 0.044 lying on an horizontal axis separated by $d = 0.066$ (b) observation on the transect lines of the dilation of Figure 1(a). Bound is equal to 0.244. (c) length distribution of the void segments of Figure 1(a), computed on the same transect lines as on Figure 1(b), together with its confidence band under independence hypothesis. Thick line : p-value of the length distribution at each distance. (d) length distribution of the void segments of Figure 1(b), together with its confidence band under independence hypothesis. Thick broken line : p-value of the length distribution at each distance.
- **Figure 2:** (a) realization of a Strauss process with intensity 24.3, inhibition parameter $c=0.5$ and inhibition distance 0.44. Same grains are attached as in Figure 1(a) (b), (c), (d) similar to Figure 1(b,c,d) with bound 0.244.
- **Figure 3:** p-values of the test based on void segment variance against p-values under independence hypothesis. Same typical point processes are used as in Figures 1(a) and 2(a). Same grains as in Figures 1(a) and 2(a) are used, but with disks separating distances varying regularly from 0.066 (thin lines) to 0.264(thick lines). Three observed window sizes were considered: (a) 450 x 450, (b) 900 x 900, (c) 1350 x 1350.
- **Figure 4:** Data examples. (a) isotropic soil surface (0.5m x 0.5m) intersection at 10cm height from the lowest point. (b) isotropic soil surface (0.5m x 0.5m) intersection at 10cm height from the lowest point. (c) box bushes repartition on a 130m x 160m area.
- **Figure 5:** segment length distribution of the void segments computed on examples 4(a,b,c) with bounds equal to 80mm, 80mm and 9m respectively.
- **Figure 6:** (a) health status of apricot trees in 4 orchards. Diseased trees are in black. (b) inter-event distance distribution of diseased trees and confidence band under independence hypothesis. (c) length distribution of void segments, chosen bound is equal to 12m.

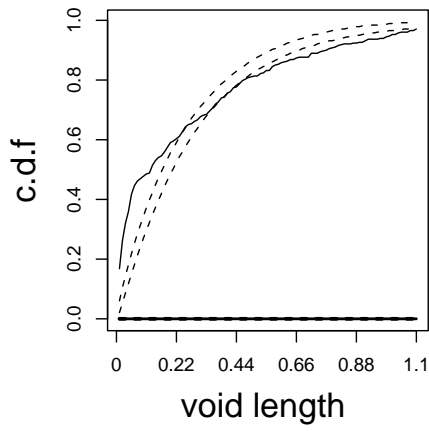


(a)



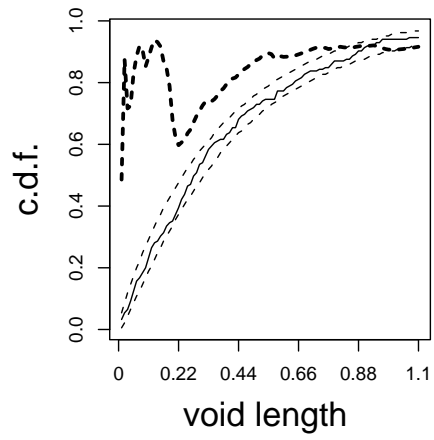
(b)

initial



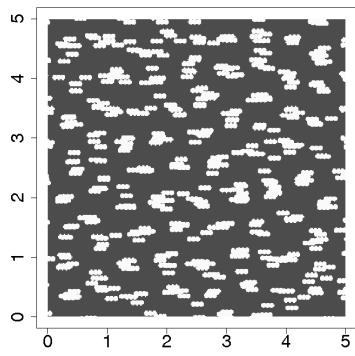
(c)

dilated

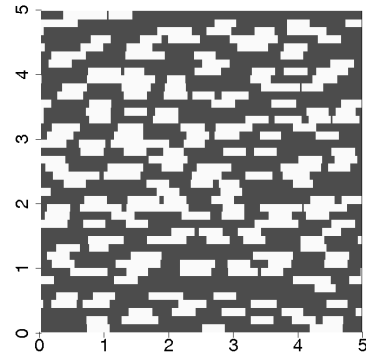


(d)

Figure 1



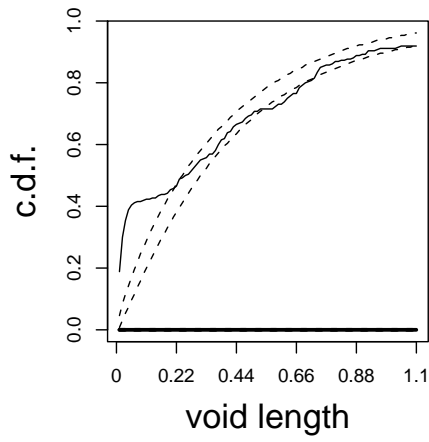
(a)



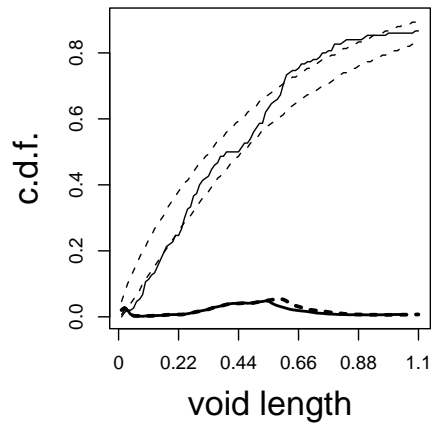
(b)

initial

dilated



(c)



(d)

Figure 2

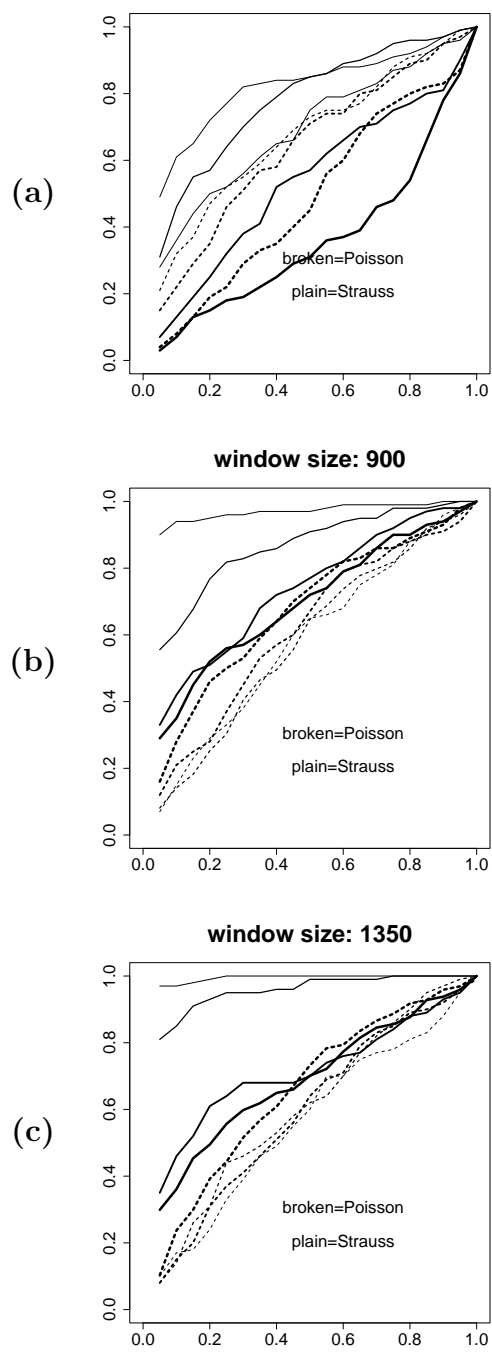


Figure 3

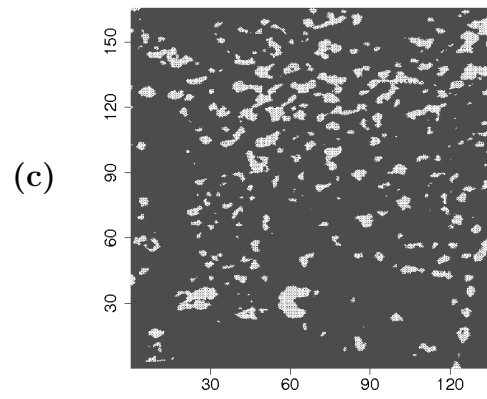
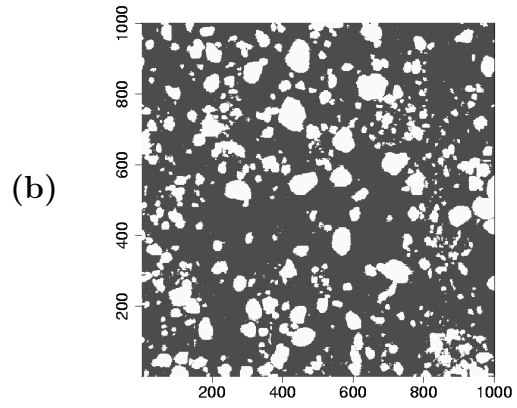
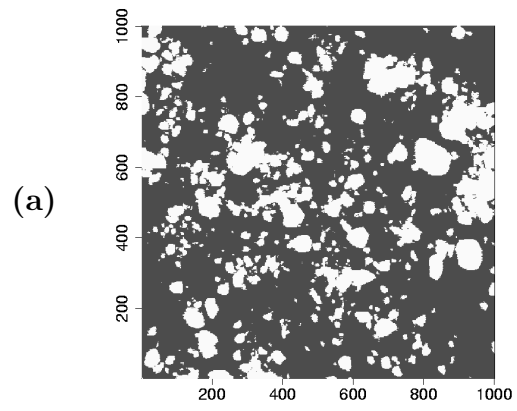


Figure 4

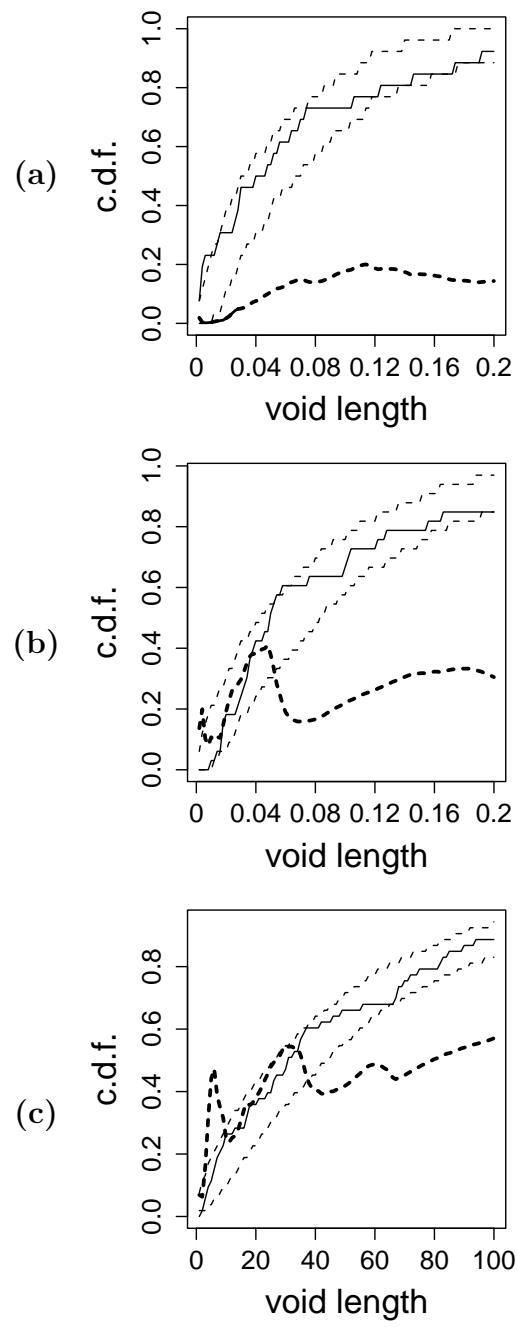


Figure 5

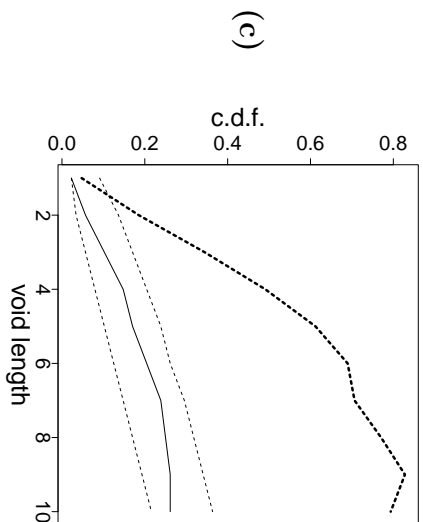
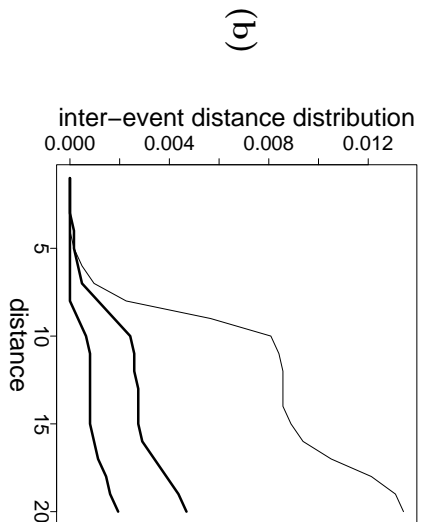
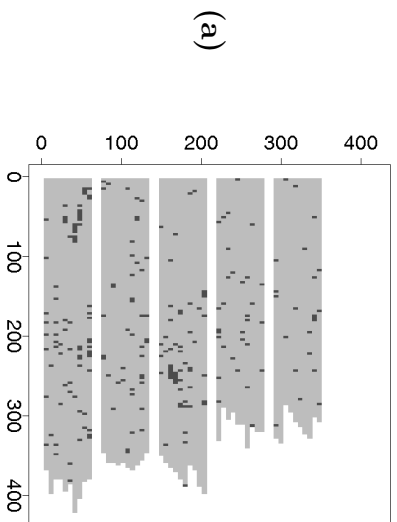


Figure 6